

# Assembly of a Nucleoprotein Complex Required for DNA Packaging by Bacteriophage $\lambda$ <sup>†</sup>

Qin Yang,<sup>‡</sup> Adrienne Hanagan,<sup>‡</sup> and Carlos Enrique Catalano<sup>\*,‡,§</sup>

Department of Pharmaceutical Sciences, School of Pharmacy, and Molecular Biology Program, School of Medicine, University of Colorado Health Sciences Center, Denver, Colorado 80262

Received September 9, 1996; Revised Manuscript Received November 19, 1996<sup>®</sup>

**ABSTRACT:** A critical step in the assembly of bacteriophage  $\lambda$  is the excision of a single genome from a concatemeric DNA precursor and insertion of genomic DNA into an empty viral capsid. DNA packaging is mediated by the  $\lambda$  proteins gpNu1 and gpA, which form an enzyme complex known as terminase. Initiation of the packaging process requires assembly of the terminase subunits onto *cos*, the  $\lambda$  DNA packaging sequence, and nicking of the duplex, thus forming the 12-base-pair “sticky” ends of the mature genome. We have utilized gel-retardation techniques to examine the interaction of gpNu1, gpA, and terminase holoenzyme with DNA. Our data demonstrate that gpNu1 interacts specifically with *cos*-containing DNA, forming three gel-retarded complexes. Similarly, the larger gpA subunit binds to DNA, forming two complexes; however, this subunit forms similar complexes with DNA substrates of random sequence. All of the nucleoprotein complexes examined are disrupted by elevated concentrations of NaCl and we suggest that altered DNA binding is responsible for the extreme salt sensitivity of the endonuclease activity of the enzyme [Tomka, M. A., & Catalano, C. E. (1993) *J. Biol. Chem.* 268, 3056–3065]. DNA binding by each subunit is strongly affected by the presence of the other, with 10- and 3-fold increases in the affinity of gpNu1 and gpA, respectively, for DNA. Moreover, our data suggest that the terminase subunits interact in solution prior to DNA binding. Finally, we provide evidence that complex I, the first stable intermediate in the packaging pathway, is composed of the mature left genome end bound to the terminase subunits and demonstrate that dissociation of the complex is quite slow ( $t_{1/2} > 8$  h). The significance of these data with respect to terminase-mediated genome packaging is discussed.

The assembly of an infectious virus particle requires the interaction of multiple proteins of both viral and host origin (Fields & Knipe, 1990). In the case of bacteriophage  $\lambda$ , the virus is assembled from preformed capsids and 48.5-kb<sup>1</sup> genomes which are excised from a concatemeric DNA precursor (Feiss, 1986; Becker & Murialdo, 1990; Murialdo, 1991; Catalano et al., 1995). Genome excision and packaging is the responsibility of an enzyme complex known as terminase which is composed of the products of the phage  $\lambda$  genes *Nu1* and *A*. Based upon data published over many years, a model describing the packaging pathway for phage  $\lambda$  has been developed (Becker & Murialdo, 1990; Murialdo, 1991; Catalano et al., 1995)<sup>2</sup> which proceeds as follows: (i) The terminase subunits gpNu1 (20.4 kDa) and gpA (72 kDa) and the *Escherichia coli* protein integration host factor (IHf)

assemble onto a multielement DNA packaging site (*cos*) forming a multiprotein pre-nicking complex. Terminase, mediated by the gpA subunit (Rubinchik et al., 1994), then introduces staggered nicks into the duplex 12 base apart, which upon strand separation yields a stable nucleoprotein complex composed of terminase bound to the mature left end of the  $\lambda$  genome ( $D_L$ ). (ii) This binary enzyme•DNA intermediate, known as complex I, next binds to an empty capsid forming a packaging intermediate known as complex II. Terminase-mediated translocation along the duplex, presumably powered by ATP hydrolysis, then results in packaging the genome within the capsid. (iii) Upon encountering the next downstream *cos* (the end of the genome), the translocating terminase complex stops and again introduces staggered nicks into the duplex. Strand separation simultaneously results in formation of the 12-base single-stranded right end of the mature  $\lambda$  genome ( $D_R$ ) and release of the DNA-filled head from the enzyme•DNA complex. In this manner, a single genome is cut from the concatemeric precursor and packaged within a viral capsid. Similar mechanisms for DNA packaging have been proposed for all of the double-stranded DNA phages and likely apply to eucaryotic viruses such as the herpesvirus groups (Casjens, 1985; Black, 1988; Roizman & Sears, 1991).

The structure of *cos* is tripartite, consisting of a nicking region (*cosN*), a “binding” region (*cosB*), and an upstream region important for termination of the packaging process (*cosQ*) [for reviews see Feiss (1986), Becker and Murialdo (1990), and Catalano et al. (1995)]. *cosN* exhibits hyphenated 2-fold rotational symmetry and the nicks introduced by

<sup>†</sup> This work was supported by National Science Foundation Grant DMB-9018767 and National Institutes of Health Grant GM50328-02.

\* Address correspondence to this author.

<sup>‡</sup> Department of Pharmaceutical Sciences.

<sup>§</sup> Molecular Biology Program.

<sup>®</sup> Abstract published in *Advance ACS Abstracts*, February 1, 1997.

<sup>1</sup> Abbreviations: bp, base pairs;  $\beta$ -ME, 2-mercaptoethanol;  $C_{1/2}$ , the concentration of a protein required to half-deplete and/or half-form a specific protein•DNA complex; *cos*, cohesive end site, the junction between individual genomes in immature concatemeric  $\lambda$  DNA; gpA, the large (72-kDa) subunit of phage  $\lambda$  terminase; gpNu1, the small (20.4-kDa) subunit of phage  $\lambda$  terminase; IHf, *Escherichia coli* integration host factor; kb, kilobase; ND-PAGE, nondenaturing polyacrylamide gel electrophoresis.

<sup>2</sup> The model for DNA packaging is presented in a concise form for the sake of brevity. Several reviews exist, however, which describe each aspect of the packaging pathway in greater detail (Becker & Murialdo, 1990; Catalano et al., 1995; Feiss, 1986; Murialdo, 1991).

terminase are displaced symmetrically within this dyad. On the basis of the symmetry of this element, it has been suggested that a catalytically competent terminase complex requires the assembly of a gpA dimer bound at *cosN* (Becker & Murialdo, 1990; Murialdo, 1991; Catalano et al., 1995). *cosB* extends from base pair (bp) 50 to 170 in the  $\lambda$  genome and consists of three 16-bp terminase recognition elements designated R1–R3 (Feiss, 1986; Murialdo, 1991; Catalano et al., 1995). Genetic studies have demonstrated that gpNu1 interactions at *cosB* are critical to viral replication (Cue & Feiss, 1992), and DNase footprinting studies have demonstrated that gpNu1 binds at the three R-elements found within *cosB* (Shinder and Gold, 1988).

It is clear that the first step in the packaging pathway is the assembly of a prenick complex at *cos*. Nicking of the duplex at *cosN*, strand separation, and prohead binding follow, all of which are mediated by the terminase subunits. Work performed in several laboratories has led to a model for DNA packaging in phage  $\lambda$  and the description of several nucleoprotein intermediates required for the packaging process [for detailed reviews, see Feiss (1986), Becker and Murialdo (1990), Murialdo (1991), and Catalano et al. (1995)]. The nature of the nucleoprotein intermediates has not, however, been rigorously defined in a biochemical sense, particularly with respect to the stoichiometry of the terminase subunits bound at *cos*. As a first step toward characterization of the interactions leading to the formation of these nucleoprotein packaging intermediates, we have investigated protein-DNA interactions of the isolated terminase subunits with *cos*-containing DNA using gel mobility shift assays. We present data which suggest that the terminase subunits interact in solution prior to binding DNA and demonstrate that additional cooperative DNA binding interactions at *cos* also occur. We further provide data which directly address the nature of complex I, a stable binary enzyme-DNA complex identified kinetically (Tomka & Catalano, 1993b) and isolated *in vivo* (Becker et al., 1977). A biochemical scheme for the assembly of a prenick complex and the transition to complex I is presented.

## EXPERIMENTAL PROCEDURES

**Materials and Methods.** Tryptone, yeast extract, and agar were purchased from Difco. Restriction enzymes and the Klenow fragment were purchased from Promega. Unlabeled nucleoside triphosphates (disodium salts) and ampicillin were purchased from Sigma Chemical Co. Radionucleotides were purchased from ICN. All other materials were of the highest quality commercially available.

**Protein Purification and DNA Preparation.** Phage  $\lambda$  terminase was purified from AZ1930 (generously provided by H. Murialdo, University of Toronto, Ontario, Canada) as described by Tomka and Catalano (1993b). The isolated terminase subunits, gpNu1 and gpA, were purified from BL21(DE3)[pCEC] and BL21(DE3)[pMAT], respectively. The gpA subunit was purified as described for terminase holoenzyme (Tomka & Catalano, 1993b), while gpNu1 was purified from inclusion bodies essentially as described by Lin and Cheng (1991). The details of the construction of these vectors and purification of the terminase subunits will be published separately (Hanagan et al., 1997). *E. coli* integration host factor was purified from HN880 (a kind gift of H. Nash, National Institutes of Health, Bethesda, MD) by the method of Nash et al. (1987). All of our purified

proteins were homogenous as determined by SDS-PAGE and densitometric analysis using a Molecular Dynamics laser densitometer and the ImageQuant data analysis package. Unless otherwise indicated, protein concentrations were determined by BCA assay (Dunn, 1994).

The plasmid pAFP1, which contains the entire *cos* sequence (*cosQ*–*cosN*–*cosB*) cloned into a pUC19 background, was purified from JM107[pAFP1] (kindly provided by M. Feiss, University of Iowa, Iowa City, IA) using Qiagen DNA prep columns. The 266-bp *cos*-containing fragment used in this study (266mer) was obtained by *EcoRI*–*HindIII* double digestion of pAFP1 and purification of the fragment by 1% agarose gel using standard methods (Maniatis et al., 1982). Unless otherwise indicated, the fragment was radio-labeled in both ends using the Klenow fragment and [ $\alpha$ - $^{32}$ P]-dATP (Maniatis et al., 1982). Specific radiolabeling of the *EcoRI* or *HindIII* end of the duplex was accomplished with [ $\alpha$ - $^{32}$ P]dTTP or [ $\alpha$ - $^{32}$ P]dGTP, respectively. A 216-bp non-specific (*cos*-minus) DNA substrate was similarly prepared by double digestion of pAFP1 and *EcoRI* and *NdeI*. The final DNA concentrations were determined by UV spectroscopy using a Hewlett-Packard HP8452A spectrophotometer (Maniatis et al., 1982).

**DNA Mobility Shift Experiments.** Unless otherwise indicated, the binding buffer used in these studies was 20 mM Tris, pH 8.0, containing 1 mM ATP, 5 mM spermidine, 1 mM EDTA, 7 mM  $\beta$ -ME, and 10% glycerol. 3'-End-labeled DNA was included at a concentration of 1 nM and protein (terminase holoenzyme, gpA, and/or gpNu1) was added as indicated in each individual experiment. The mixtures (10  $\mu$ L) were kept at room temperature for 20 min and then loaded (neat) onto a 5% polyacrylamide gel (acrylamide:bisacrylamide ratio of 80:1). The gels were run in 0.5 $\times$  TBE at 10 V/cm for 2 h and dried onto Whatman 3MM filter paper and the dried gels analyzed using a Molecular Dynamics personal phosphorimager and the ImageQuant software package.

**Data Analysis.** Where single apparent binding transitions were observed, the raw data were fit to the following logistical sigmoidal curve function:

$$\% \text{ complex} = \left[ \frac{(m_x + b_x) - (m_n + b_n)}{1 + \left( \frac{[\text{protein}]}{C_{1/2}} \right)^{m_s}} + (m_n + b_n) \right] \quad (1)$$

where  $m_x/m_n$  and  $b_x/b_n$  represent the slopes and y-intercepts of the maximum and minimum baselines, respectively,  $m_s$  represents the slope of the curve within the transition region, and  $C_{1/2}$  represents the midpoint (inflection point) of the curve. In those situations where two apparent transitions were observed, the raw data were fit to the following double-sigmoidal curve function:

$$\% \text{ complex} = \left[ \left( \frac{B_{x-A} - B_{n-A}}{1 + \left( \frac{[\text{protein}]}{C_{1/2-A}} \right)^{m_{s-A}}} + B_{n-A} \right) + \left( \frac{B_{x-B} - B_{n-B}}{1 + \left( \frac{[\text{protein}]}{C_{1/2-B}} \right)^{m_{s-B}}} + B_{n-B} \right) \right] \quad (2)$$

where  $B_{x-A}/B_{x-B}$  and  $B_{n-A}/B_{n-B}$  represent the maximum and

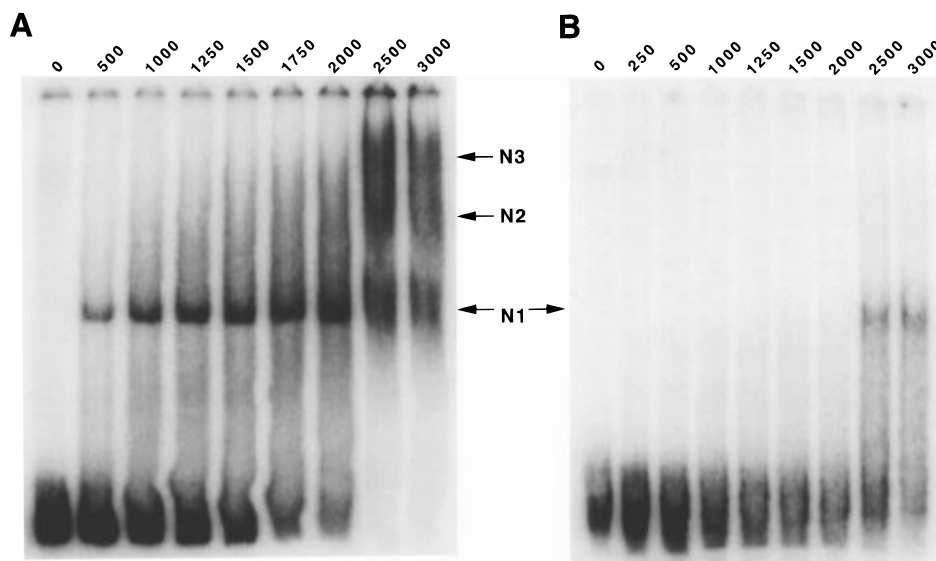


FIGURE 1: gpNu1 binds specifically to *cos*-containing DNA. Purified gpNu1 protein was added at the indicated nanomolar concentrations to *cos*-containing (panel A) or nonspecific (panel B) DNA and the protein·DNA complexes were fractionated by ND-PAGE as described in Experimental Procedures. The nucleoprotein complexes N1–N3 are indicated with arrows.

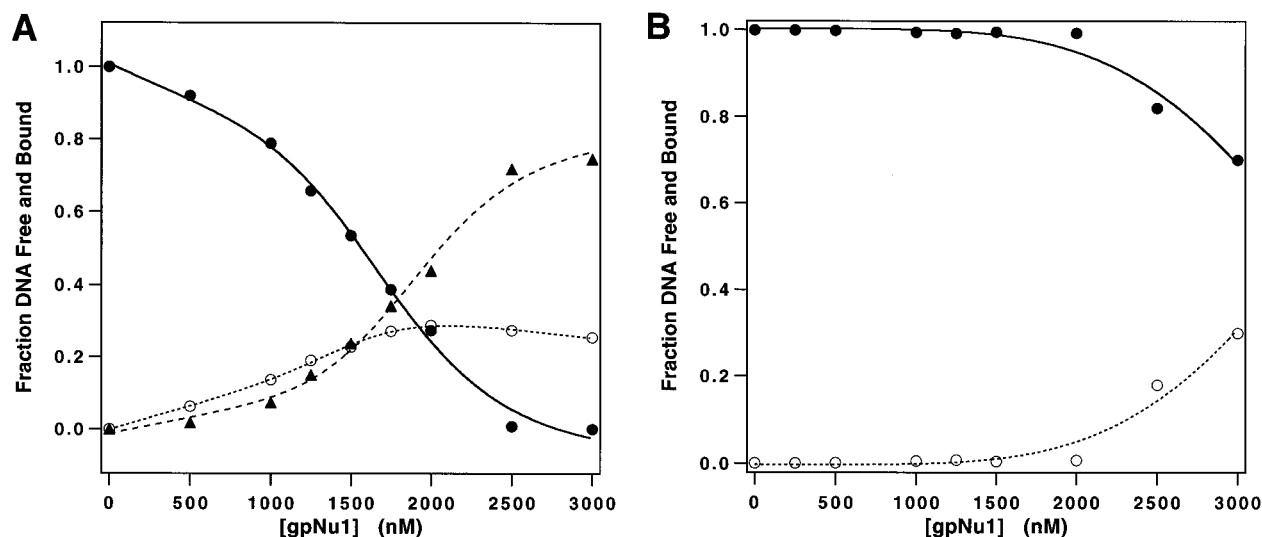


FIGURE 2: Quantitation of gpNu1 binding to DNA. The gel retardation data were quantitated as described in Experimental Procedures and are presented as the fraction of the total DNA present in each of the indicated complexes. Each data point is the average of three separate experiments. Panel A: The fraction of *cos*-containing DNA (specific substrate) found free in solution (●), in the N1 complex (○), and in N2 plus N3 complexes (▲) are shown. Complexes N2 and N3 appeared simultaneously and were quantitated as a single entity. The solid, dotted, and dashed lines represent the best fit of the free DNA, complex N1, and complexes N2/N3 data, respectively, to eq 1. The  $C_{1/2}$  values determined from each curve are presented in Table 1. Panel B: The fraction of nonspecific (random sequence) DNA found free in solution (●) and as a gel-retarded complex (○).

minimum baselines for the individual transitions (A and B), respectively,  $m_{s-A}/m_{s-B}$  represents the slope of the curve within the individual transition regions, and  $C_{1/2-A}/C_{1/2-B}$  represents the midpoint (inflection point) of each individual curve. The indicated constants were determined by nonlinear regression analysis of the experimental data using the Igor data analysis program (Wave Metrics, Lake Oswego, OR) as described previously (Tomka & Catalano, 1993a).

In both of the above equations,  $C_{1/2}$  mathematically represents the concentration of protein required to half-deplete (or half-form) a specific complex and thus provides a crude approximation of the relative binding affinities of proteins for DNA (Carey, 1991). In all cases, where  $C_{1/2}$  values were determined using the above equations, the concentration of DNA was less than 0.2% of the calculated protein concentration.

## RESULTS

### Interaction of the Isolated Terminase Subunits with DNA.

Interaction of the terminase gpNu1 subunit with DNA was examined by gel mobility assay as described in Experimental Procedures. Figure 1 shows that gpNu1 binds with relative specificity of *cos*-containing DNA, yielding three complexes (N1, N2, and N3). Analysis of these data demonstrates that the N1 complex is formed in a linear fashion with increasing concentrations of gpNu1 and over a wide concentration range (Figure 2). The slower migrating N2/N3 complexes are also detected at the lower protein concentrations and are similarly formed in a linear fashion. These upper complexes are comparatively unstable, however, and do not form sharp, well-resolved bands (see Figure 1). This pattern of retardation behavior is typical of weak protein·DNA complexes

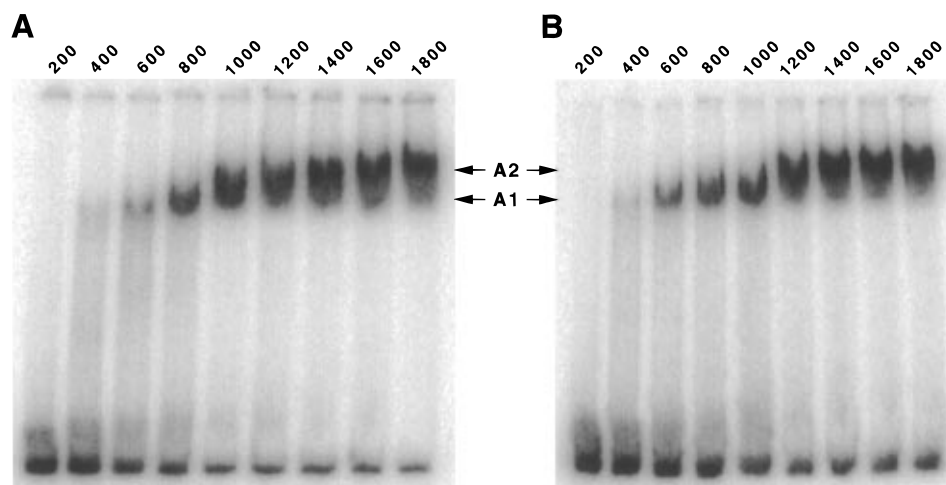


FIGURE 3: gpA binds to *cos*-containing and nonspecific DNA. Purified gpA protein was added at the indicated nanomolar concentrations to *cos*-containing DNA (panel A) and nonspecific DNA (panel B) and the protein·DNA complexes fractionated by ND-PAGE. The nucleoprotein complexes A1 and A2 are indicated with arrows.

(Carey, 1991). As the concentration of gpNu1 is further increased ( $>2000$  nM), discrete N2 and N3 complexes appear simultaneously and over a very narrow concentration range. Analysis of the data according eq 1 yields a  $C_{1/2}$  value of  $\approx 1700$  nM for the formation of the N1 complex and  $\approx 2000$  nM for the formation of complexes N2 and N3 (Table 1). We note that stable N2/N3 complexes appear at a concentration where gpNu1 also interacts with nonspecific DNA (see Figure 1).

Figure 3 demonstrates that the terminase gpA subunit binds to *cos*-containing DNA yielding two complexes of reduced mobility (A1 and A2).<sup>3</sup> Unlike gpNu1, however, the isolated gpA subunit also binds reasonably well to nonspecific DNA. Moreover, identical gel retardation patterns were observed with both *cos*-containing and nonspecific DNA, suggesting that gpA binds in a similar manner to both duplexes. The initial interaction forming complex A1 appears to be relatively nonspecific, as reflected by virtually identical  $C_{1/2}$  values for both *cos*-containing and nonspecific DNA (Figure 4, Table 1). Some discrimination may be apparent in subsequent formation of complex A2, however, with  $C_{1/2}$  values of 835 and 1085 nM for *cos*-containing and nonspecific DNA, respectively (Figure 4, Table 1). A modest level of discrimination for *cos*-containing DNA is also evident from direct competition experiments which demonstrate that DNA with a *cos* site competes more effectively than DNA of random sequence (data not shown).

**Cooperative Binding of the Terminase Subunits to DNA.** Figure 5A demonstrates that binding of gpNu1 to *cos*-containing DNA is strongly stimulated by the presence of the gpA subunit, with a  $\approx 10$ -fold decrease in  $C_{1/2}$  (Table 2). We note that the concentration of gpA used in this experiment (500 nM) yields only modest binding to *cos*-containing DNA (see Figure 3). Similarly, low concentrations of the terminase gpNu1 subunit stimulate binding of gpA to *cos*-containing DNA  $\approx 3$ -fold (Figure 5B, Table 1). As in the

previous experiment, the concentration of gpNu1 used (500 nM) only modestly bound DNA when present alone (see Figure 1). That the binding curves for each subunit in the presence of the other are quite similar suggests that the same species is interacting with *cos*-containing DNA in each instance. The gpNu1 subunit also stimulated gpA binding to nonspecific DNA, although less strongly ( $\approx 1.5$ -fold, not shown). These data suggest that gpNu1·gpA protein·protein interactions stimulate gpA binding to DNA, at least in part, without the need for gpNu1 binding to *cosB*. Finally, we note that binding of gpNu1 in the presence of gpA yields multiple retarded complexes with *cos*-containing DNA (but not nonspecific DNA, data not shown). Importantly, these slower migrating complexes appear at a concentration of gpNu1 which is in excess of the gpA. Taken together, these data suggest that the gpNu1 subunit binds to *cos*-containing DNA both alone and as a gpA·gpNu1 protein complex.

**Effect of  $Mg^{2+}$ , ATP, and NaCl on DNA Binding.** Interactions of the terminase gpA subunit with DNA were not significantly affected by the presence of  $Mg^{2+}$  and/or ATP (Table 3). Similar results were obtained with the gpNu1 subunit as long as either  $Mg^{2+}$  or ATP was present in the binding buffer. Exclusion of both compounds, however, resulted in a dramatic decrease in the ability of the protein to bind DNA with the virtual absence of any detectable gpNu1·DNA complexes (Table 3).

The gpNu1·DNA complexes are differentially sensitive to salt. While the N2/N3 complexes are essentially nonexistent at a NaCl concentration greater than 100 mM (Figure 6A), the N1 complex appears relatively stable and, in fact, persists at salt concentrations as great as 500 mM (data not shown). The concentration of gpNu1 in the above experiment was relatively high, however, to allow the formation of the slower migrating complexes, and the N1 complex is similarly salt-sensitive when the protein concentration is decreased (Figure 6B). Figure 6C demonstrates that the gpA·DNA complexes are also sensitive to elevated concentrations of NaCl. Consistent with the modest level of discrimination for *cos*-containing DNA in the binding experiments described above, the complexes formed with *cos*-containing DNA appear slightly more stable than those formed with nonspecific DNA. Finally, Figure 6D demonstrates that the gel-retarded complexes formed with terminase

<sup>3</sup> We note that resolution of the complexes was not complete. Attempts to increase the separation between the observed bands by using different acrylamide:bisacrylamide concentrations and longer gels were uniformly unsuccessful. Nevertheless, analysis of several experiments consistently and reproducibly demonstrated the presence of two complexes which were formed in a protein concentration-dependent manner.

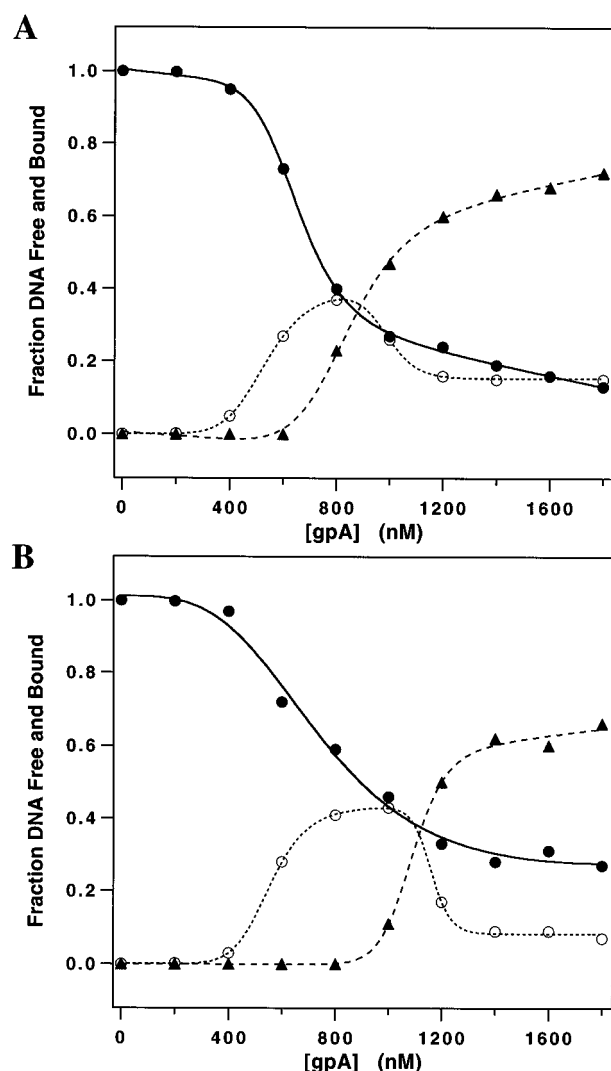


FIGURE 4: Quantitation of gpA binding to DNA. The gel retardation data were quantitated as described in Experimental Procedures and are presented as the fraction of the total DNA present in each of the indicated complexes. Each data point is the average of three separate experiments. The symbols denote the fraction of *cos*-containing DNA (panel A) and nonspecific DNA (panel B) found free in solution (●), in complex A1 (○), and in complex A2 (▲). The solid and dashed lines represent the best fit of the free DNA and complex A2 data, respectively, to eq 1. The dotted line represents the best fit of the complex A1 data to eq 2. The  $C_{1/2}$  values determined from each curve are presented in Table 1.

Table 1: Quantitation of gpNu1 and gpA Binding to DNA<sup>a</sup>

protein added	complex formed	$C_{1/2}$ (nM) for <i>cos</i> -containing DNA	$C_{1/2}$ (nM) for nonspecific DNA
gpNu1	N1 <sup>b</sup>	1715 ± 117	NE <sup>c</sup>
gpNu1	N2/N3 <sup>b</sup>	2045 ± 117	NE
gpA	A1 <sup>d</sup>	540 ± 11	560 ± 14
gpA	A2 <sup>b</sup>	835 ± 19	1085 ± 19

<sup>a</sup> The data presented in Figures 2 and 4 were analyzed as described in Experimental Procedures yielding the  $C_{1/2}$  values (± standard deviation) presented in the table. <sup>b</sup>  $C_{1/2}$  value calculated using eq 1. <sup>c</sup> NE, not examined. <sup>d</sup>  $C_{1/2}$  value calculated using eq 2.

holoenzyme are also quite sensitive to the concentration of salt included in the binding buffer. These data are consistent with our prior demonstration that the endonuclease activity of the enzyme was strongly inhibited by concentrations of NaCl greater than 100 mM and support our earlier suggestion

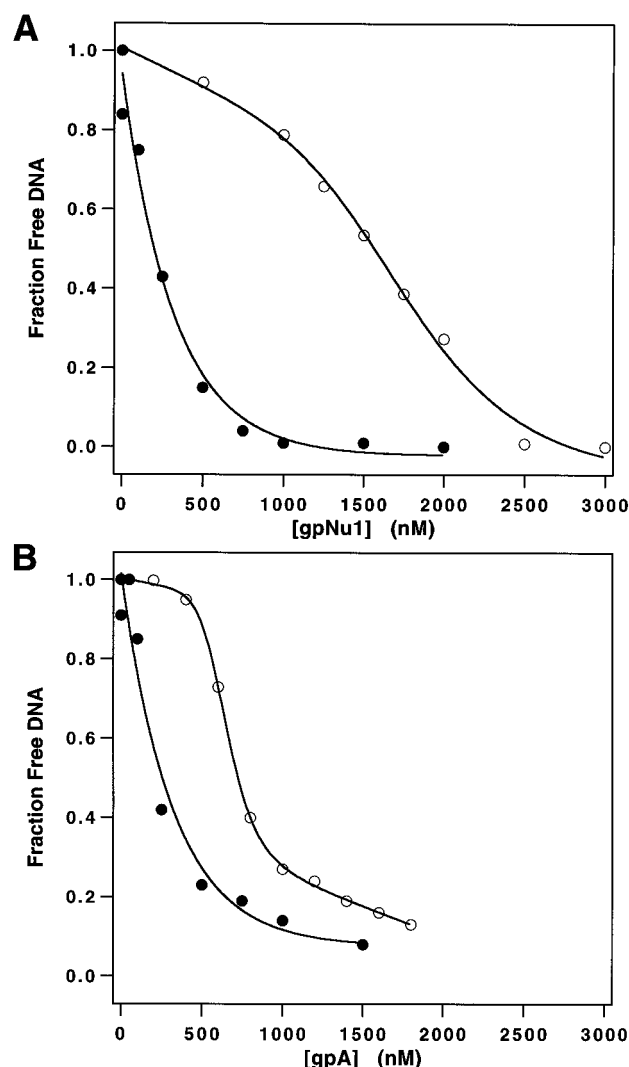


FIGURE 5: Interaction of the terminase subunits stimulates DNA binding. Panel A: Binding of purified gpNu1 to *cos*-containing DNA was examined in the absence (○) and presence (●) of 500 nM gpA as described in Figure 1. The fraction of DNA found free in solution is displayed in each case. Panel B: Binding of purified gpA to *cos*-containing DNA was examined in the absence (○) and presence (●) of 500 nM gpNu1 as described in Figure 3. As in panel A, the fraction of DNA found free in solution displayed. Each data point is the average value of two separate experiments.

Table 2: Interaction of the Terminase Subunits Stimulates DNA Binding<sup>a</sup>

protein added	$C_{1/2}$ (nM)
gpNu1	1940 ± 120 <sup>b</sup>
gpNu1 (+500 nM gpA)	≈200 <sup>c</sup>
gpA	650 ± 10 <sup>b</sup>
gpA (+500 nM gpNu1)	≈200 <sup>c</sup>

<sup>a</sup> The data presented in Figure 5 were analyzed as described in Experimental Procedures yielding the  $C_{1/2}$  values presented in the table.

<sup>b</sup>  $C_{1/2}$  value (± standard deviation) calculated using eq 1 as described.

<sup>c</sup>  $C_{1/2}$  values estimated from the data presented in Figure 5.

that this was due to impaired binding to *cos*-containing DNA (Tomka & Catalano, 1993b).

**Nature of Complex I.** Initial assembly of the terminase subunits at *cos* yields the pre-nicking complex poised to hydrolyze the DNA duplex at *cosN*. Nicking of the duplex ultimately yields complex I, a stable enzyme·DNA intermediate first characterized *in vivo* (Becker et al., 1977) and subsequently demonstrated in kinetic experiments *in vitro*

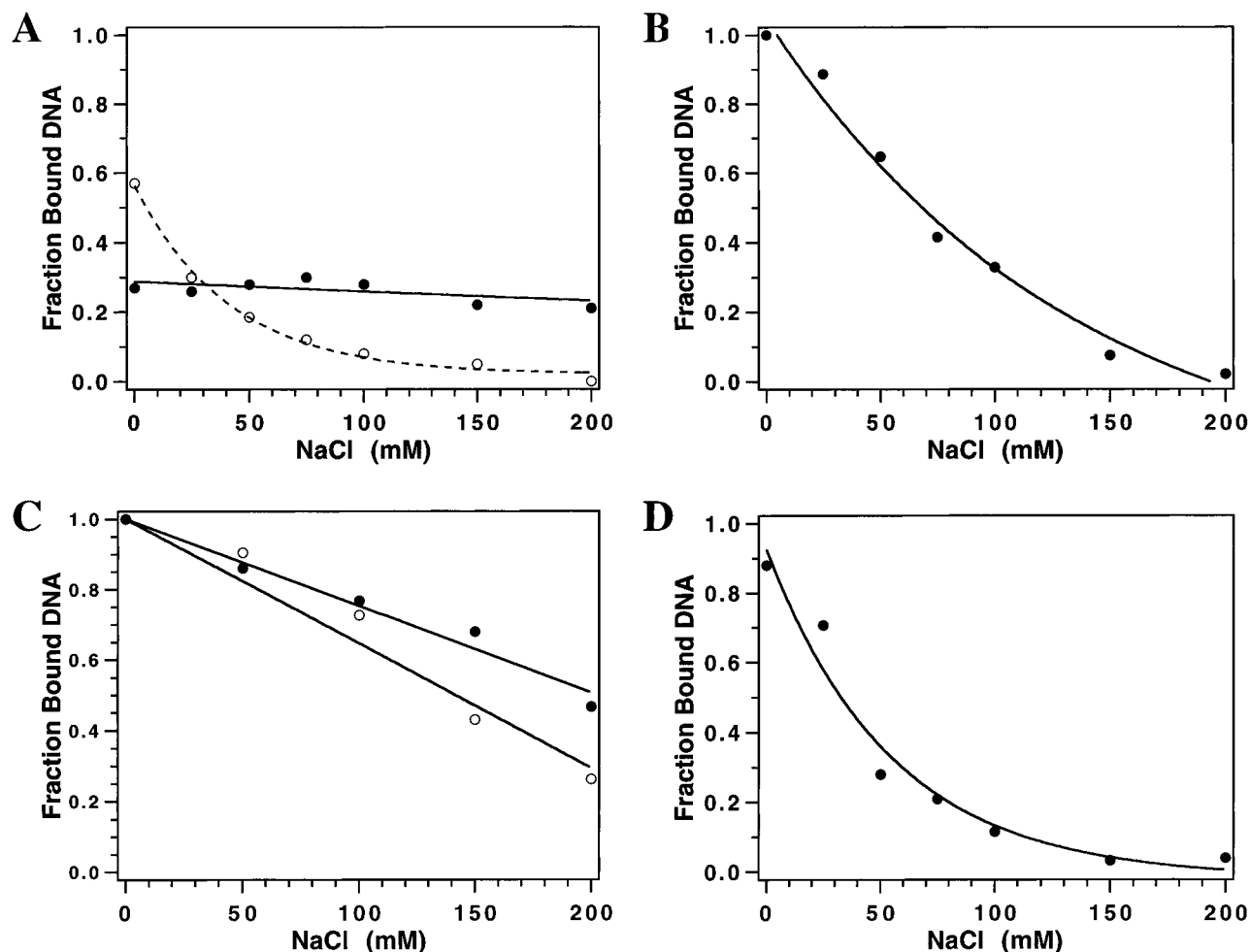


FIGURE 6: Effects of salt on binding of the terminase subunits to DNA. The gpNu1 terminase subunit was added to 1500 nM (panel A) or 500 nM (panel B) and the fraction of DNA present as the N1 complex (●) and as N2/N3 complexes (○) quantitated as described in Experimental Procedures. The gpA subunit was added to 600 nM (panel C) in the presence of *cos*-containing (●) or nonspecific (○) DNA and the fraction of total DNA present as gel-retarded complexes determined as described. Terminase holoenzyme was included at a concentration of 300 nM (panel D) and the fraction of DNA present in gel-retarded complexes displayed. In every case, each data point is the average of two separate experiments.

Table 3: Magnesium and ATP Dependence of DNA Binding<sup>a</sup>

protein	MgCl <sub>2</sub>	ATP	% retarded complex
gpA	+	+	80
gpA	—	+	70
gpA	—	—	80
gpNu1	+	+	44
gpNu1	—	+	42
gpNu1	—	—	ND <sup>b</sup>

<sup>a</sup> The isolated gpA (1000 nM) and gpNu1 (1500 nM) subunits were incubated with *cos*-containing DNA and the percentage of DNA present as gel-retarded complexes was quantitated as described in Experimental Procedures. Mg<sup>2+</sup> and ATP were included at 10 and 1 mM, respectively, as indicated in the table. <sup>b</sup> ND, no gel-retarded complexes could be detected by phosphorimager analysis.

(Tomka & Catalano, 1993b; Catalano & Tomka, 1995). While *in vivo* data suggest that complex I consists of terminase bound to the strand-separated mature left end of the  $\lambda$  genome [Sippy & Feiss, 1992; Kuzminov et al., 1994; also cited in Murialdo (1991)], the nature of the kinetically identified binary enzyme•DNA intermediate remains obscure. We have therefore examined the mobility shift of DNA by terminase holoenzyme in the presence of both Mg<sup>2+</sup> and ATP, a situation where cleavage of the duplex occurs. In this experiment, *cos*-containing DNA was specifically ra-

diolabeled in either the left genome end (D<sub>L</sub>, *Eco*RI end labeled) or the right genome end (D<sub>R</sub>, *Hind*III end labeled) as described in Experimental Procedures (see Figure 7A). Cleavage of the DNA at *cos* yields the matured  $\lambda$  genomic ends, D<sub>L</sub> and D<sub>R</sub>, 190 and 76 bp in length, respectively. Figure 7B demonstrates that, under conditions where the duplex is fully digested, the D<sub>L</sub> fragment remains associated with the enzyme subsequent to duplex nicking with no radiolabeled duplex observed free in solution. Heating of the sample results in disruption of the protein•DNA complex and release of the radiolabeled fragment, confirming that strand nicking has indeed occurred. Conversely, the D<sub>R</sub> fragment is not associated with terminase in a gel-retarded complex subsequent to strand scission but is rather observed as free DNA (Figure 7B). These data demonstrate that complex I comprises terminase and the mature left end of the  $\lambda$  genome formed by enzyme-mediated duplex nicking and strand separation, thus releasing D<sub>R</sub>. Interestingly, Figure 7C demonstrates that both the pre-nicking complex and complex I are quite stable and persist for hours in the presence of a vast excess of competitor DNA. Analysis of these data yield dissociation rate constants ( $k_{off}$ ) of  $9.8 \times 10^{-4} \text{ min}^{-1}$  ( $t_{1/2} = 11.7 \text{ h}$ ) and  $1.4 \times 10^{-3} \text{ min}^{-1}$  ( $t_{1/2} = 8.1 \text{ h}$ ) for the pre-nicking complex and complex I, respectively.

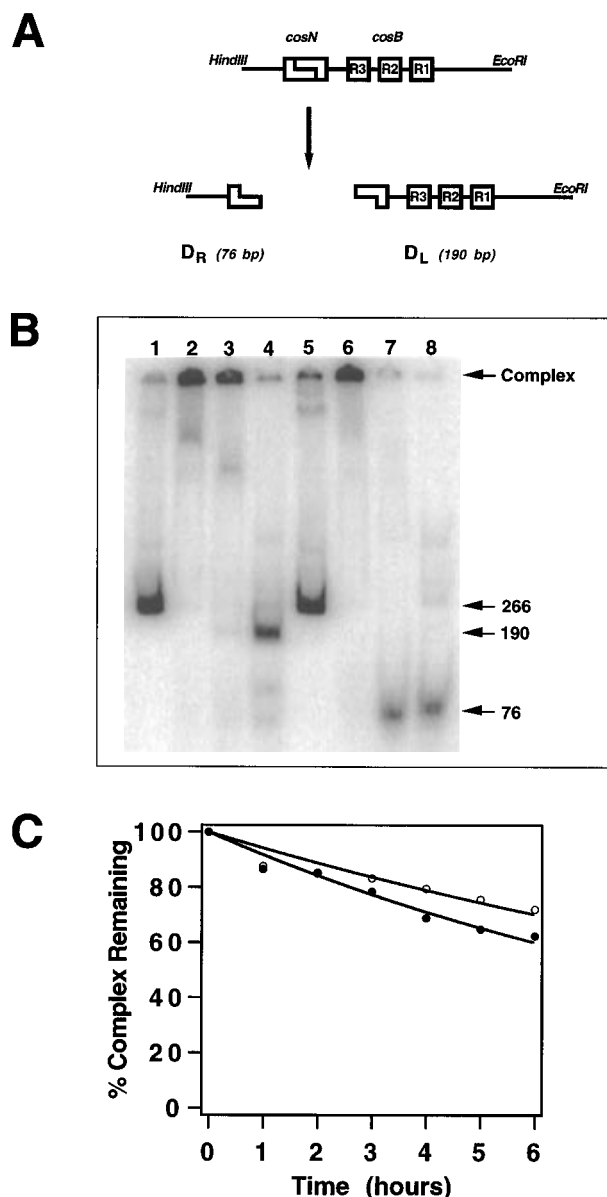


FIGURE 7: Nature of complex I. Panel A: Terminase-mediated cleavage of the 266mer *cos*-containing DNA substrate yields the mature phage  $\lambda$  genome ends,  $D_R$  and  $D_L$ , 76 and 190 bp in length, respectively. Panel B: Terminase was incubated with *EcoRI* end-labeled (lanes 1–4) or *HindIII* end-labeled (lanes 5–8) 266mer and the gel-retarded complexes were analyzed as described. Specific radiolabeling of the *EcoRI* and *HindIII* end of the DNA substrate was accomplished as described in Experimental Procedures. The binding buffer used in each reaction was as described with the following modifications: lanes 1 and 5, no enzyme; lanes 2 and 6, 700 nM terminase holoenzyme was added in the absence of  $Mg^{2+}$ ; lanes 3 and 7, 700 nM terminase holoenzyme was added in the presence of 10 mM  $Mg^{2+}$ ; lanes 4 and 8, 700 nM terminase holoenzyme was added in the presence of 10 mM  $Mg^{2+}$  and the samples were heated to 70 °C for 5 min prior to loading on the gel. The binding mixtures were kept at 37 °C for 20 min and then loaded onto the resolving gel as described in Experimental Procedures. The location of the DNA substrate and the *cos* cleavage fragments are indicated with arrows. Panel C: Terminase holoenzyme (700 nM) was preincubated with *cos*-containing DNA for 20 min in the absence (○) or presence (●) of  $Mg^{2+}$  as described in Experimental Procedures. A 100-fold molar excess of unlabeled competitor DNA (unlabeled 266mer) was then added and the mixtures were further incubated at 4 °C. Aliquots were removed at the indicated times and analyzed for the presence of gel-retarded complexes as described. The solid lines represent the best fit of the data to an exponential decay function and were used to determine the dissociation rate constants ( $k_{off}$ ) presented in the text.

## DISCUSSION

The enzyme responsible for genome packaging in bacteriophage  $\lambda$  is terminase. As a first step toward characterization of the packaging intermediates, we have utilized gel mobility shift assays to investigate the interaction of the terminase subunits with *cos*, the packaging site in the  $\lambda$  genome. We have shown that the two terminase subunits interact differentially with DNA. The small gpNu1 subunit binds with relatively specificity to *cos*-containing DNA, forming three complexes in a concentration-dependent manner. While our data do not allow us to define the nature of the observed complexes at the molecular level, three models may be proposed to explain the data. (1) Given the tendency of the gpNu1 protein to aggregate in solution (Parris et al., 1988; Tomka & Catalano, 1993b; Hanagan et al., 1997), it is possible that the N1 complex results from binding of a gpNu1 protomer<sup>4</sup> to *cosB* while the N2 and N3 complexes represent interactions with higher-order gpNu1 solution oligomers. (2) Alternatively, the N1 complex may result from specific interactions with *cos* while the slower migrating complexes represent binding of additional gpNu1 proteins to DNA in a nonspecific manner. This model is consistent with the observation that the slower migrating species appear at a protein concentration which is sufficient for nonspecific binding to DNA and with the salt sensitivity of the N2 and N3 complexes. Implicit in this model is the concept that the N1 complex may, in fact, be an ensemble of nucleoprotein complexes representing gpNu1 proteins bound at each of the R-elements found within *cosB*. (3) A final model suggests that the three complexes observed result from specific gpNu1 binding at each of the three R-elements found within *cosB* (Figure 8, part A). While our data do not allow us to rigorously prove either model, we favor the last model for the following reasons. First, DNase footprinting studies have demonstrated binding of gpNu1 to each of the individual R-elements at concentrations similar to those used in the studies reported here (Shinder & Gold, 1988; Parris et al., 1994). This suggests that the three complexes observed in our studies represent gpNu1 proteins similarly bound to each of the three binding sites. Second, experiments presented here have demonstrated that the gpNu1 subunit stimulates gpA binding to both specific and non-specific DNA, although the extent of stimulation is greater with *cos*-containing substrates. At elevated gpNu1 concentrations, however, additional complexes of slower mobility appear when *cos*-containing DNA is used which are absent with nonspecific DNA (data not shown). These data demonstrate that *cosB*, the binding site for gpNu1, is required for these additional interactions and suggest that binding is specific for the R-elements. Within the context of the model, the N1 complex may thus represent gpNu1 interactions with the R3 DNA binding element while the less stable N2/N3 complexes result from additional interactions with the R2 and R1 elements (Figure 8, part A). This follows from the demonstration that R3 is the dominant element for both *cos*

<sup>4</sup> Few data are available on the concentration-dependent solution oligomerization of the purified gpNu1 subunit. Parris et al. (1994) have suggested that gpNu1 exists in solution as an apparent dimer, while experiments conducted in our laboratory suggest that the purified gpNu1 subunit interconverts between an apparent tetramer and hexamer depending on buffer composition (Hanagan et al., 1997). We thus utilize the term protomer to describe the most elementary gpNu1 oligomerization state (monomer, dimer, etc.).

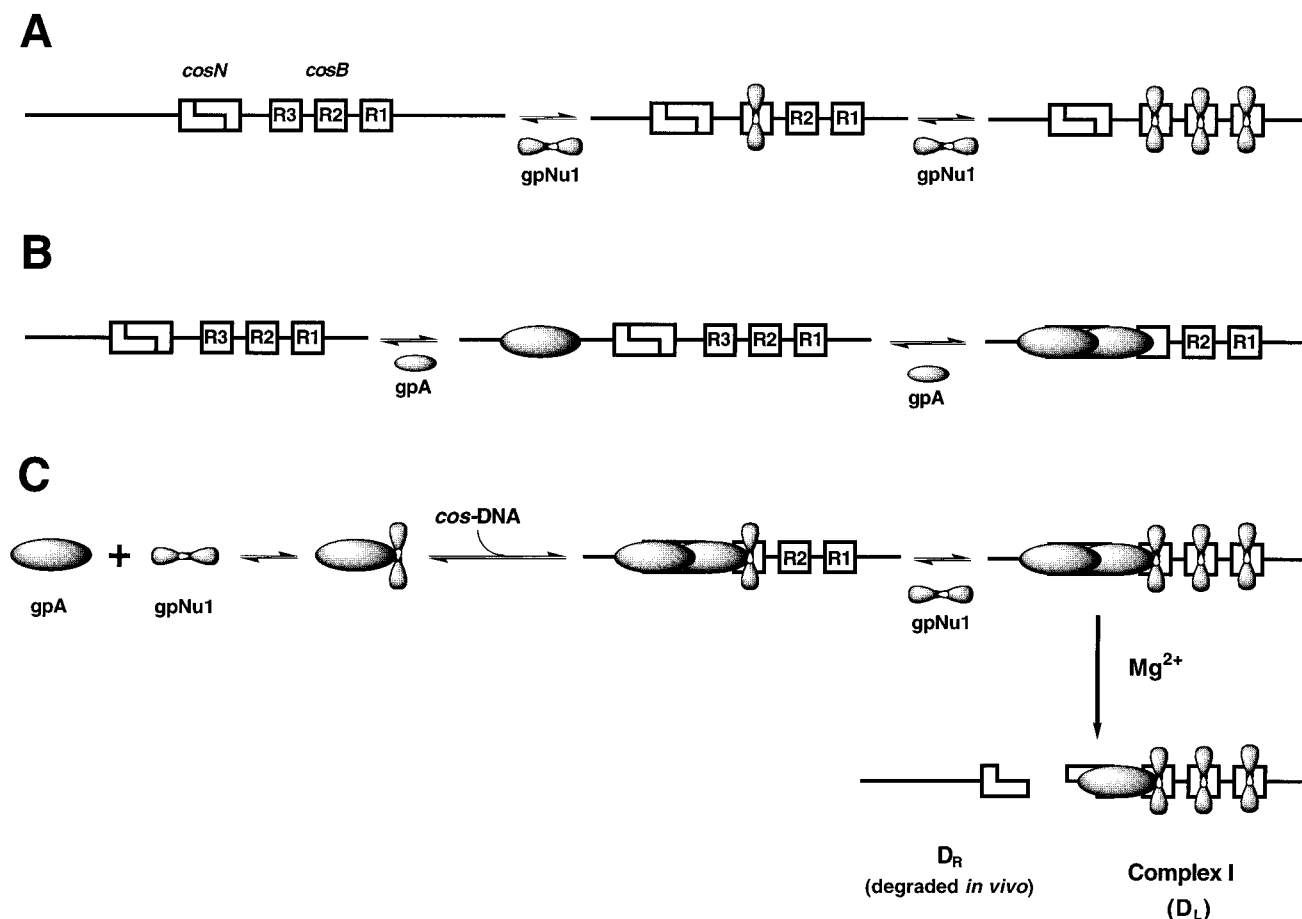


FIGURE 8: Biochemical scheme for terminase assembly at *cos* and the TER reaction. Shown in the proposed scheme for gpNu1 (panel A), gpA (panel B), and terminase holoenzyme (panel C) binding to *cos*-containing DNA. This biochemical scheme is based upon previously published models for terminase assembly at *cos* (Becker & Murialdo, 1990; Catalano et al., 1995; Murialdo, 1991) and the data presented here. We note that no direct evidence exists which describes the subunit stoichiometry of terminase bound to DNA. Moreover, relatively little information exists as to the solution oligomerization state of the isolated terminase subunits (see footnotes 4 and 5). The model presented is not meant to imply a detailed knowledge of the subunit stoichiometry of the nucleoprotein complexes observed in this work. Details of the model are presented in the text.

cleavage and *in vivo* DNA packaging with the R2 and R1 elements playing only modulatory roles (Cue & Feiss, 1993; Higgins & Becker, 1994; Higgins et al., 1988). We finally note that the scheme presented in Figure 8 is consistent with the putative role of the gpNu1 subunit in DNA packaging, cooperative assembly of a gpA dimer at *cosN* (Feiss, 1986; Murialdo, 1991; Catalano et al., 1995).

It has long been suspected that gpA binds to *cosN* as a symmetrically disposed homodimer (Feiss, 1986; Becker & Murialdo, 1990; Murialdo, 1991; Catalano et al., 1995), and we suggest that the A1 and A2 gel-retarded complexes represent monomeric<sup>5</sup> and dimeric gpA nucleoprotein complexes (Figure 8, part B). We note, however, that gpA binds reasonably well to DNA of random sequence and that similar complexes are formed with both *cos*-containing and non-specific DNA. These data suggest that gpA does not strictly require *cosN* for assembly. Nevertheless, some specificity for *cos* is evident in the formation of A2, suggesting that formation of the "dimeric" complex involves, at least in part, direct interactions between gpA and *cosN*.

<sup>5</sup> Few data are available on the concentration-dependent solution oligomerization of the purified gpA subunit. We thus utilize the term gpA monomer to describe the most elementary oligomerization state of the protein and that protein species which interacts with DNA to form complex A1, (see footnote 4).

DNA binding by each of the terminase subunits is strongly affected by the presence of the other, with a shift in the observed  $C_{1/2}$  toward significantly lower protein concentrations. Moreover, the binding curves for each subunit in the presence of the other are quite similar and suggest that the same species is interacting with *cos*-containing DNA in each instance. Isolation of terminase holoenzyme from *E. coli* yields a gpA<sub>1</sub>•gpNu1<sub>2</sub> heterotrimer (Gold & Becker, 1983; Tomka & Catalano, 1993b; Parris et al., 1994) that is insensitive to salt, suggesting strong protein•protein interactions in solution. Taken together, these data suggest that when both subunits are present, the terminase subunits interact to form an oligomeric protein complex prior to DNA binding.

Subsequent to the initial assembly of the pre-nicking complex, terminase-mediated nicking of the duplex ultimately leads to the formation of complex I, a stable intermediate in the packaging pathway. The most direct evidence for the nature of this complex has come from *in vivo* experiments with packaging-deficient virus. DNA isolated from *E. coli* infected with these defective phage yield matured genome left ends (D<sub>L</sub>) but no detectable matured right ends (D<sub>R</sub>) [Sippy & Feiss, 1992; Kuzminov et al., 1994; also cited in Murialdo (1991)]. This has been interpreted as protection of the left end by the terminase complex



subsequent to strand separation and release of the genome right end into solution. The single-stranded right end thus formed would be rapidly degraded *in vivo* and would not be detectable. We have previously identified a stable enzyme•DNA intermediate in the kinetic analysis of the *cos* cleavage reaction and have related this biochemical complex to the *in vivo* defined complex I (Tomka & Catalano, 1993b; Catalano & Tomka, 1995). The nature of the kinetically defined complex was not well-defined, however. We have directly examined the macromolecular nature of complex I using a gel mobility assay. In the absence of divalent metal, a nucleoprotein preniking complex assembles onto DNA yielding a gel-retarded complex containing both ends of the original duplex. Our data clearly demonstrate that in the presence of  $Mg^{2+}$ , conditions which result in strand scission, a stable complex is formed which consists of terminase bound to the matured left genome end ( $D_L$ ) resulting from strand separation and release of  $D_R$ .

**Biochemical Scheme for Terminase-Mediated DNA Packaging.** On the basis of published information and the data presented here, we propose the following model for the assembly of a terminase preniking complex and the formation of complex I (Figure 8, part C). The gpA and gpNu1 subunits interact in solution to form a  $gpA_1 \cdot gpNu1_2$  protein complex which binds specifically to *cos*-containing DNA. The terminase heterotrimer is specific for *cos* by virtue of gpNu1 binding to the *cosB* R3 element and to a lesser extent by direct gpA•*cosN* interactions. This is consistent with the demonstration by Becker and colleagues that the R3 element is both necessary and sufficient for terminase holoenzyme binding to *cos* and nicking of the duplex (Higgins et al., 1988; Higgins & Becker, 1994). At sufficient concentrations of gpNu1, additional interactions at the R2 and R1 elements further stabilize the complex. We suggest that these additional interactions become increasingly important as terminase•*cos* interactions become weakened, i.e., by mutation and/or limiting protein/DNA concentrations. Once assembled at *cos*, the preniking complex is poised to nick the duplex strands upon binding of  $Mg^{2+}$ , yielding the nicked, annealed complex. Subsequent strand separation and release of the  $D_R$  fragment, presumably driven by ATP hydrolysis, yields compound I, the first stable intermediate in the packaging pathway.

The transition from preniking complex to a strand-separated nucleoprotein intermediate (complex I) to a rapidly translocating DNA packaging machine (complex II) is most certainly accompanied by a significant reorganization of the multiprotein complexes assembled at *cos*. While it is clear that both of the terminase subunits are required for the formation of complex I, the subunit composition of each of the above intermediates remains a mystery.<sup>6</sup> On the basis of our data, however, we suggest that the gpNu1 subunit is part of and is required for the stability of complex I. Strong

site-specific binding is detrimental to translocation, however, and it is likely that gpNu1 must, at least in part, release DNA prior to active genome packaging. Conversely, the efficient binding of gpA to nonspecific DNA is an ideal property for a translocating complex and gpA may in fact be the ATPase "machine" driving DNA packaging. This investigation represents our preliminary endeavors to define the nature of each of the nucleoprotein intermediates involved genome packaging by bacteriophage  $\lambda$ . A detailed mechanistic understanding of the protein•protein and protein•DNA interactions leading to each of the catalytically competent packaging complexes must, however, await further investigation.

## ACKNOWLEDGMENT

We thank Drs. David Bain, Michael Feiss, and Robert Kuchta for helpful discussions and critical review of the manuscript.

## REFERENCES

- Becker, A., et al. (1977) *Virology* 78, 291–305.
- Becker, A., & Murialdo, H. (1990) *J. Bacteriol.* 172, 2819–2824.
- Black, L. W. (1988) DNA Packaging in dsDNA Bacteriophages, in *The Bacteriophages*, (Calendar, R., Ed.) pp 321–373, Plenum Publishing Corp., New York.
- Carey, J. (1991) *Methods Enzymol.* 208, 103–118.
- Casjens, S. A. (1985) An Introduction to Virus Structure and Assembly, in *Virus Structure and Assembly* (Casjens, S. A., Ed.) pp 1–28. Jones and Bartlett Publishers, Inc., Boston, MA.
- Catalano, C. E., & Tomka, M. A. (1995) *Biochemistry* 34, 10036–10042.
- Catalano, C. E., et al. (1995) *Mol. Microbiol.* 16, 1075–1086.
- Cue, D., & Feiss, M. (1992) *J. Mol. Biol.* 228, 58–71.
- Cue, D., & Feiss, M. (1992) *J. Mol. Biol.* 228, 72–87.
- Dunn, M. J. (1994) Determination of Total Protein Concentration, in *Protein Purification Methods, A Practical Approach* (Harris, E. L. V., & Angal, S., Eds.) pp 10–17. IRL Press, New York.
- Feiss, M. (1986) *Trends Genet.* 2, 100–104.
- Fields, B. N., & Knipe, D. M. (1990) General Virology, Introduction, in *Fields Virology* (Fields, B. N., & Knipe, D. M., Eds.) pp 3–9, Raven Press, New York.
- Gold, M., & Becker, A. (1983) *J. Biol. Chem.* 258, 14619–14625.
- Hanagan, A., et al. (1997) *Biochemistry* (submitted for publication).
- Higgins, R., & Becker, A. (1994) *EMBO J.* 13, 6152–6161.
- Higgins, R. R., et al. (1988) *Cell* 54, 765–775.
- Kuzminov, A., et al. (1994) *EMBO J.* 13, 2764–2776.
- Lin, K.-H., & Cheng, S.-Y. (1991) *BioTechniques* 11, 748–751.
- Maniatis, T., et al. (1982) *Molecular Cloning, A Laboratory Manual*, Cold Spring Harbor Laboratory Press, Cold Spring Harbor, NY.
- Murialdo, H. (1991) *Annu. Rev. Biochem.* 60, 125–153.
- Nash, H. A., et al. (1987) *J. Bacteriol.* 169, 4124–4127.
- Parris, W., et al. (1988) *J. Biol. Chem.* 263, 8413–8419.
- Parris, W., et al. (1994) *J. Biol. Chem.* 269, 13564–13574.
- Roizman, B., & Sears, A. E. (1991) *Fundamental Virology* (Fields, B. N., et al., Eds.) 2nd Ed., pp 863–865. Raven Press, New York.
- Rubinchik, S., et al. (1994) *J. Biol. Chem.* 269, 13575–13585.
- Shinder, G., & Gold, M. (1988) *J. Virol.* 62, 387–392.
- Sippy, J., & Feiss, M. (1992) *J. Bacteriol.* 174, 850–856.
- Tomka, M. A., & Catalano, C. E. (1993a) *Biochemistry* 32, 11992–11997.
- Tomka, M. A., & Catalano, C. E. (1993b) *J. Biol. Chem.* 268, 3056–3065.

BI9622682

<sup>6</sup> Currently accepted models for terminase-mediated DNA packaging assume that the terminase subunit(s) are part of the translocating complex and likely form the DNA packaging "machine". There is, however, no direct evidence for participation of either of the terminase subunits in this process.